Available online at www.sciencedirect.com
SCIENCE DIRECT
Journal of Power Sources 156 (2006) 253–259
JOURNAL OF POWER SOURCES
www.elsevier.com/locate/jpowsour

Silicon-based miniaturized-reformer for portable fuel cell applications

Oh Joong Kwon, Sun-Mi Hwang, Jin-Goo Ahn, Jae Jeong Kim *

Research Center for Energy Conversion and Storage, School of Chemical and Biological Engineering, Seoul National University, Shillim-dong, Kwanak-gu, Seoul 151-742, South Korea

Received 23 March 2005; accepted 8 June 2005
Available online 18 August 2005

Abstract

A micro-reformer was made by using silicon fabrication technology and a new catalyst loading method of 'fill-and-dry coating'. The techniques of silicon wet etching, bonding and thin-film deposition were applied in the micro-reformer process, and a commercial Cu-ZnO-Al_2O_3 catalyst served as the reforming catalyst. The volume of the single micro-reactor was 0.55 cm^3 and the micro-reformer stack, which consists of one vaporizer and two reformers, occupied 15 cm^3. Methanol solution was used as the reactant and the composition and feed rate were varied. The operating temperature of the reformer was in the range of 280–320 °C and was controlled by an electrical thin-film heater at a fixed vaporizer temperature of 150 °C. The product gas was composed of 75% H_2, 25% CO_2 and 2100 ppm CO. The maximum hydrogen production rate and conversion were about 200 cm^3 and 95% at 320 °C, respectively.

Keywords: Miniaturized-reformer; Silicon technology; Catalyst coating; Hydrogen generation

1. Introduction

The fuel cell is on its way to becoming compact and portable to provide an alternative to batteries that are unsatisfactory energy sources for evolving portable electronic devices such as notebooks, personal digital assistants and cellular phones. Many new technologies for miniaturizing fuel cells have been researched to accomplish the same performance as a conventional fuel cell [1–7]. Although the major focus has been directed towards miniaturization of the fuel cell, the peripheral auxiliaries of a system take up more space than the fuel cell itself. Among such peripheral auxiliaries, hydrogen storage occupies the largest space. Thus, miniaturization of the fuel supply component is no less important than that of fuel cell. This paper deals with this subject.

Four types of hydrogen supply methods, namely compressed hydrogen, chemical hydride, metal hydride and reformed hydrogen have been generally used for polymer electrolyte membrane fuel cells (PEMFCs). Among these methods, reformed hydrogen is considered to have the greatest potential for portable fuel cells, due to the high energy density, fast response time, low production cost and easy refuelling. Thus, the key for applying reformed hydrogen to a portable fuel cell is how to make the reformer compact.

Micro electro mechanical systems (MEMSs) and silicon technology are promising technologies for miniaturizing conventional macro-scale facilities into compact devices. Accordingly, there are much research into bioMEMS, microactuators, micro-sensors and micro-reactors [8–11]. The concept of the miniaturization of conventional reformers belongs to the technology of micro-reactors. Various fabrication technologies such as lithography, silicon wet etching [12], anodic bonding [13] and thin-film deposition have been adopted from the silicon process, and fabrication of the main body of the micro-reformer has been successfully accomplished with these technologies.

In addition to fabrication of main body of the reactor, catalyst loading in the micro-reformer is a critical issue. The packed-bed loading method is very popular for macro-scale reactors [14–16]. It is not suitable, however, for loading a catalyst into a micro-reactor due to the high pressure drop

* Corresponding author. Tel.: +82 2 880 8863; fax: +82 2 888 2705.
E-mail address: jjkimm@snu.ac.kr (J.J. Kim).

0378-7753/$ – see front matter © 2005 Elsevier B.V. All rights reserved.
doi:10.1016/j.jpowsour.2005.06.024

and inherent fabrication problems. Thus, other methods such as physical vapour deposition (PVD) [17] and dip coating [18,19] have been proposed along with a modified packed-bed. We have devised a 'fill-and-dry coating' procedure to load the catalyst into a preassembled micro-reformer. With a micro-reformer made by MEMS technology and the fill-and-dry coating method, the methanol steam-reforming reaction was performed.

2. Fabrication

A schematic diagram of the micro-reformer fabrication process is given in Fig. 1. A (1 1 0) silicon wafer was used to make a rectangular-shaped micro-channel by anisotropic wet etching with KOH solution. The micro-channels were 600 μm in width and 240 μm in depth (Fig. 1(a)).

An etched silicon wafer was bonded with Pyrex by anodic bonding (Fig. 1(b)). Then, an alumina layer was coated on the inside of the channel as an adhesion layer using an alumina sol prepared by the Yoldas process [20], see Fig. 1(c). The micro-channels of the pre-assembled micro-reformer were filled with alumina sol, which was pushed out by air and then dried for a day. Calcination was carried out at 500 °C.

The catalyst was loaded as a layer on the alumina coated micro-channels by means of a fill-and-dry coating method (Fig. 1(d)). A commercial Cu-ZnO-Al_2O_3 reforming catalyst from Süd-Chemie was used in all experiments. Two types of catalyst slurry were prepared with solvents of deionized (D.I.) water and alumina sol by using a ball-milling method. The alumina-coated channels were filled with either type of slurry, then dried for a day and calcined at 300 °C.

After catalyst coating, a thin-film heater was deposited by direct current (dc) magnetron sputtering on the silicon side of the micro-reformer to control the temperature during reaction (Fig. 1(e)). The thin-film heater was composed of three components, namely, TaN_x heating material, a tantalum adhesion layer, and a gold contact pad. Using the thin-film heater and a relay controlled by a proportional–integral–differential (PID) program, the temperature of the micro-reformer was precisely controlled within 0.3% accuracy up to 400 °C. The single micro-reformer fabrication was completed with deposition of the thin-film heater.

A vaporizer, connected in series to the reformer, had the same structural shape as the micro-reformer but lacked Al_2O_3 and catalyst layers. To prevent methanol vapour from condensing at the junction of the of vaporizer and the reformer, a Viton O-ring and a stainless-steel end-plate were applied (Fig. 1(f)). Photographs of the fabricated micro-reformer and stack are given in Fig. 2. The volume of the single reactor and a reformer stack composed of one vaporizer and two reformers was 0.55 and 15 ml, respectively.

3. Experimental

A schematic diagram of the complete experimental setup for activity measurements is shown in Fig. 3. A PID algorithm programmed by LabVIEW controlled the temperature of the micro-reformer during the reduction and reforming reactions. Prior to the analysis of activity, the Cu-ZnO-Al_2O_3 catalyst was reduced with 2 cm^3 of H_2 and 20 cm^3 of N_2 at 300 °C for 3 h.

Activity measurements of the alumina sol-based catalyst and the D.I. water-based catalyst were performed at a temper-

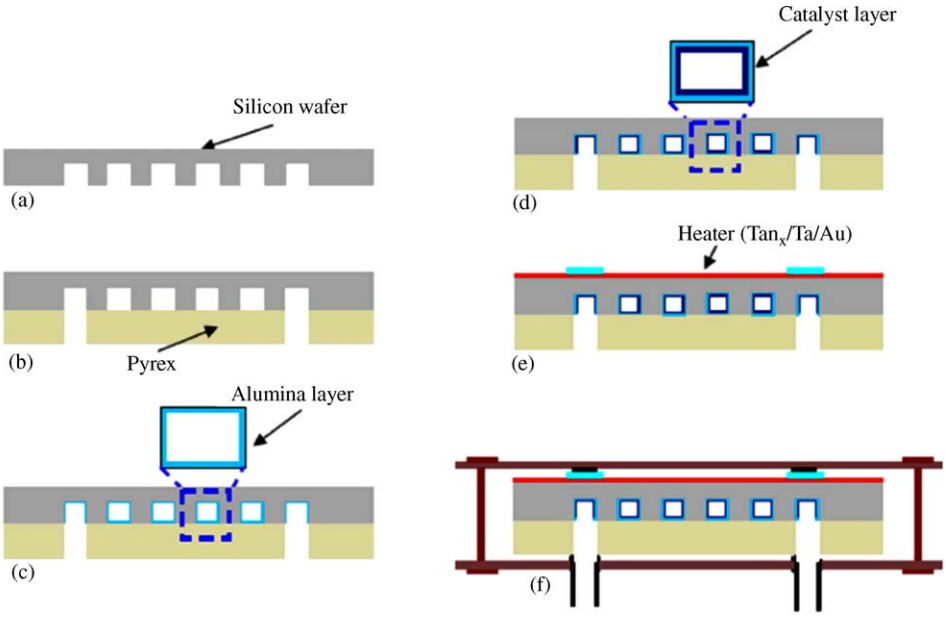

Fig. 1. Micro-reformer fabrication process: (a) silicon wet etching; (b) anodic bonding with Pyrex; (c) alumina layer coating; (d) catalyst coating; (e) thin-film heater deposition; (f) packaging with stainless-steel end-plates.

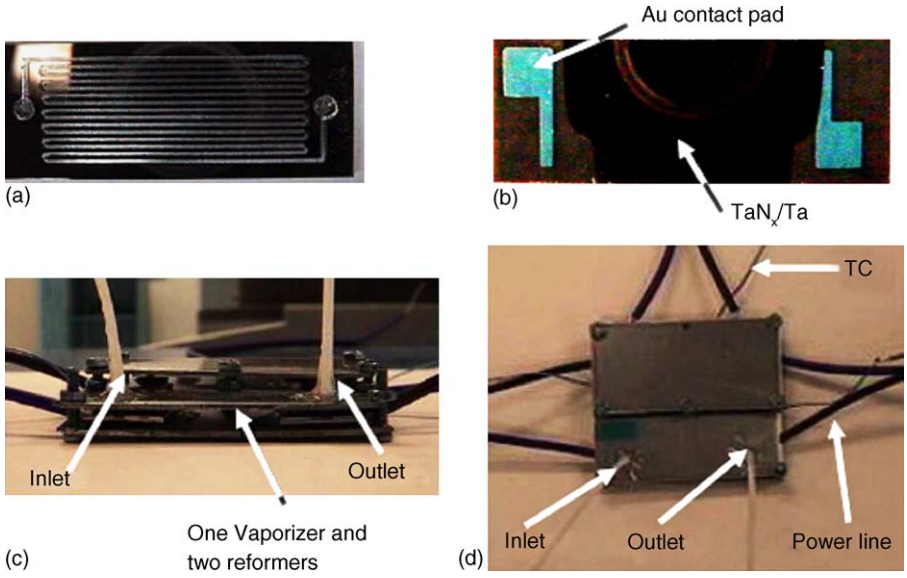

Fig. 2. Micro-reformer: (a) front side of single reactor; (b) back side of single reactor; (c) side view of reformer stack; (d) top view of reformer stack.

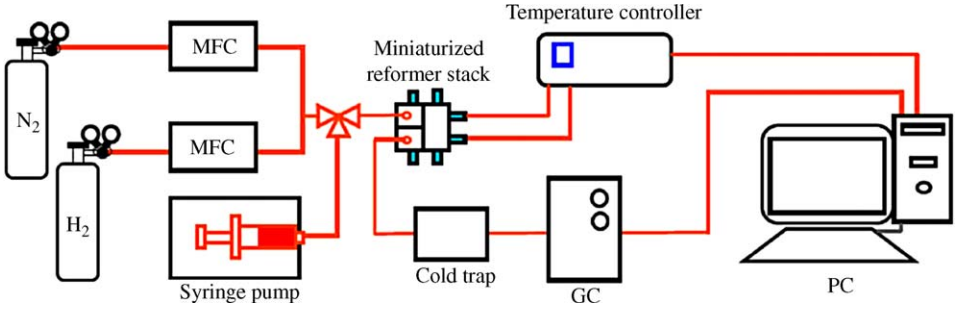

Fig. 3. Experimental setup.

ature of 150 °C for the vaporizer and 280 °C for the reformer. The American Society for Testing and Materials (ASTM) tape test and field emission scanning electron microscopy (FESEM) were employed to evaluate the effectivness of the alumina layer as an adhesion layer. A flow meter was used to measure and compare the gas production rates of the two different catalysts.

After selecting the better catalyst between the alumina sol-based and D.I. water-based catalysts, the effects of the flow rate of feed and the operation temperature on activity and production gas composition were analyzed. Micro-GC equipment (Varian CP 4900) was used for this purpose.

4. Results and discussion

To control the temperature of the micro-reformer, a Ta-based thin-film heater was introduced. The structure of the thin-film heater used in this study is shown in Fig. 4(a). The compound TaN_x saved as the main heating material and was formed on a silicon substrate. Thermal pretreatment resulted in a Ta_2O_5 passivation layer on top of the TaN_x heater. Thus, it prevented degeneration of the TaN_x heater and induced a large voltage drop. On heating, the temperature of micro-reformer with a Ta_2O_5 layer was 20 °C higher than that without Ta_2O_5 for the same power consumption. The gold contact pad also increased the temperature of the micro-reformer by 40 °C compared with that for a micro-reformer with only a thermal pretreatment step, by reducing contact resistance. With the introduction of a thermal pretreatment step and a gold contact pad, the efficiency of the thin-film heater could be increased about 23%, as shown in Fig. 4(b). The temperature of the micro-reformer could be controlled to within 0.3% with the thin-film heater.

Another key issue for the micro-reformer was how to load the catalyst on the silicon-based micro-channels. For this purpose, both a fill-and-dry coating method for catalyst coating and wash coating for the alumina adhesion layer were introduced. The alumina layer was coated on the inside of the micro-channels by filling alumina sol into the micro-channel and then the excessive sol was removed with air. Through calcination it at 500 °C, a well-coated micro-channel was

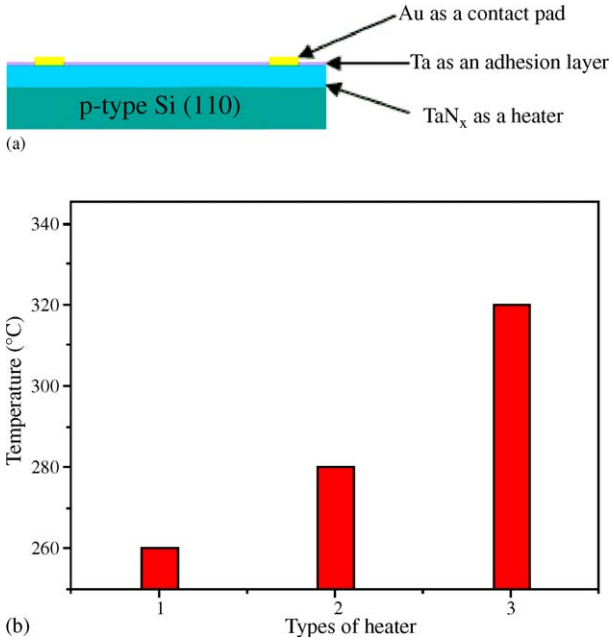

Fig. 4. (a) Structure of thin-film heater; (b) temperature of heater depending on heater types (1) as-deposited TaN_x; (2) thermally pretreated TaN_x; (c) with Au electrode.

obtained, as shown in Fig. 5(a). Detachment phenomena, signifying poor adhesion, were not observed even at the corner of the coated micro-channel. After loading the catalyst on the alumina layer, the steam-reforming reaction was performed. Without the alumina layer, the catalyst layer became loose and even peeled off at the corner after the reforming reaction. Therefore, it is clear that the alumina layer contributed to the improvement in adhesion between the substrate and the catalyst.

The photographs in Fig. 5 demonstrate that the fill-and-dry coating method renders a catalyst coating with a good loading profile. It is thought that the surface tension in the slurry dry step induces a hollow profile of catalyst adhesion on the channel wall.

After coating the catalyst over the alumina adhesion layer, the activity of the catalyst was tested at 280 °C with 1 $cm^3\ h^{-1}$ methanol solution (steam-to-carbon ratio (S/C) = 1) and various catalyst preparation methods. As mentioned above, two types of catalyst namely, an alumina sol-based catalyst and a D.I. water-based catalyst, were used. The difference between the two catalysts lies in the solvent used for the catalyst slurry. Since the alumina sol strengthens the bonding between the catalyst particles and the alumina layer, the alumina sol-based catalyst exhibits good adhesion. On the other hand, most of the catalyst particles are covered with the alumina sol and therefore the surface area exposed to reactants is reduced, as illustrated in Fig. 6(a). By contrast, the D.I. water-based catalyst has a high surface area, because the solvent used for the catalyst slurry evaporates during drying and calcination.

The dependence of activity on the catalyst preparation and coating methods is demonstrated in Fig. 6(c). The alumina-based catalyst sustains a gas production rate that is inde-

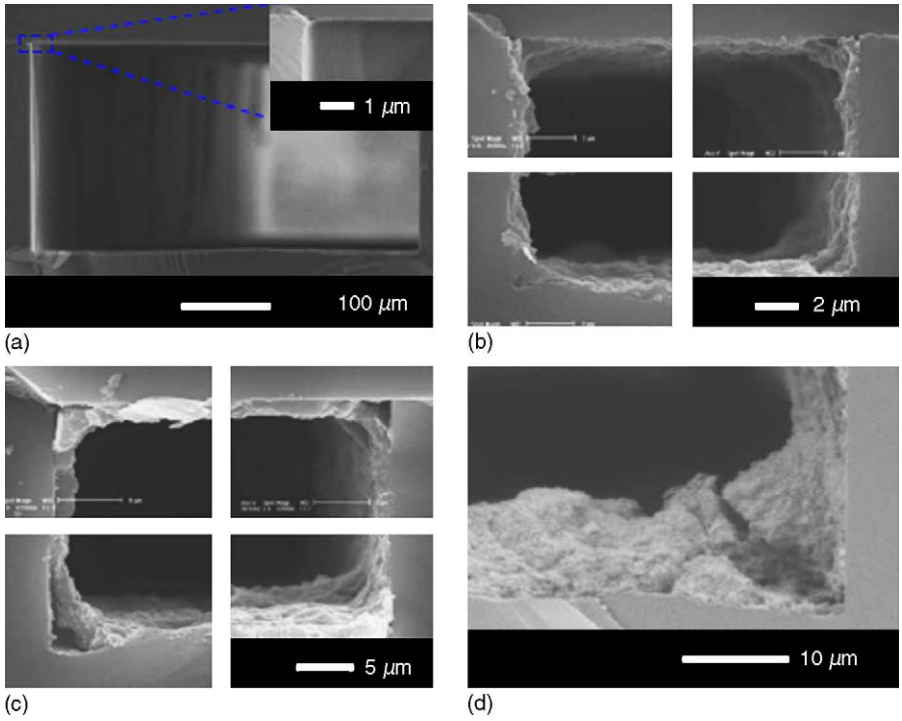

Fig. 5. Alumina layer and catalyst layer coating profile: (a) alumina layer profile; (b) catalyst layer with alumina layer; (c) catalyst layer without alumina layer; (d) D.I. water-based catalyst by fill-and-dry method.

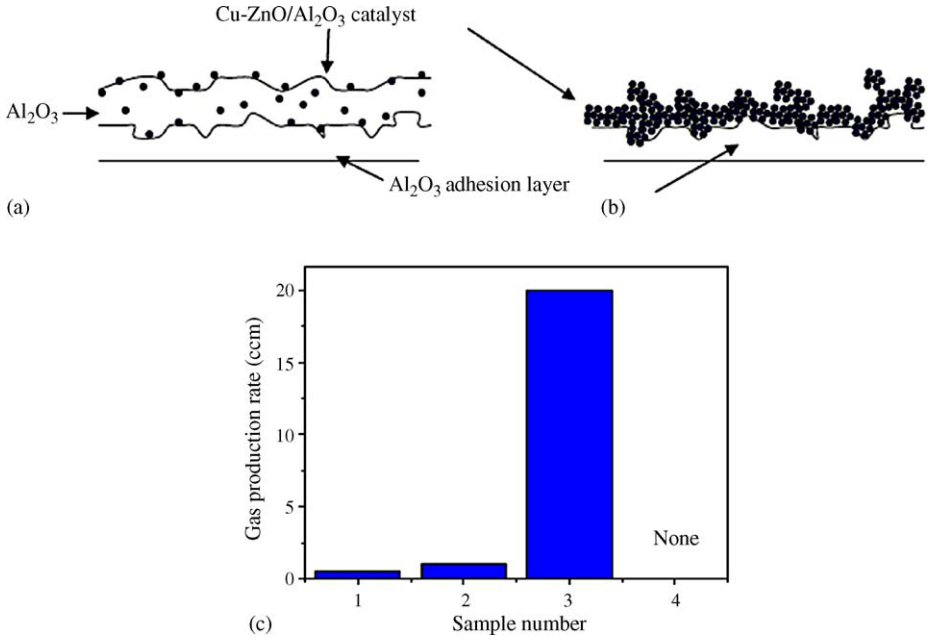

Fig. 6. Gas production rate as function of catalyst coating conditions: (a) catalyst prepared with alumina sol; (b) catalyst prepared with water; (c) gas production rate (1) alumina sol-based catalyst by fill-and-dry method; (2) alumina sol-based catalyst by wash coating method; (3) water-based catalyst by fill and dry method; (4) water-based catalyst by wash coating.

pendent of the catalyst coating method. This is because the surface area exposed to reactants is virtually unchanged. The D.I. water-based catalyst prepared by 'wash coating' was swept out during the air washing process and thus there was no gas production. The maximum gas production rate was obtained with a D.I. water-based catalyst coated by the fill-and-dry coating method. This catalyst also showed good adhesion after drying and calcination and there by could sustain the shear stress during the reforming reaction, as indicated in Fig. 5(d). The D.I. water-based catalyst coated by a fill-and-dry coating method is found to be the most effective for hydrogen generation among the four preparation methods. Accordingly, a micro-reformer stack was made with the D.I. water-based slurry to test the activity.

To investigate the effect of feed rate on the gas production rate and conversion, the methanol feed rate was varied from 1 to 10 $cm^3\,h^{-1}$ at the reformer temperature of 280 °C. To calculate the conversion from methanol to hydrogen, unreacted methanol and water vapour were removed through a cold trap that was inserted between the outlet of the micro-reformer and the inlet of the gas chromatograph analyzer. As the methanol feed rate is increased, the gas production rate increases from 28 cm^3 (hydrogen 21 cm^3) to 145 cm^3 (hydrogen 108.7 cm^3) but the conversion decreases, as shown in Fig. 7. One hundred percent conversion was observed up to 2 $ml\,h^{-1}$ feed rate, whereas it was reduced to 50.3% at the feed rate of 10 $ml\,h^{-1}$. The reduction in conversion over 3 $ml\,h^{-1}$ methanol feed rate seemed to be originated from the contact time of reactants with catalyst.

Fig. 8 shows the dependency of gas production rate and conversion on the reformer operation temperature. At a fixed methanol feed rate of 10 $cm^3\,h^{-1}$, the temperature was varied between 280 and 320 °C. The rate of gas production is 145 cm^3 (hydrogen 108.7 cm^3) at 280 °C and 275 cm^3 (hydrogen 206 cm^3) at 320 °C, while conversions is 50.3 and 95.4% at 280 and 320 °C, respectively. A hydrogen production rate of 206 cm^3 corresponds to a power output of 20 W, when 100% hydrogen utilization and a potential of 0.7 V are assumed. It is obvious that the gas production rate and conversion will increase if the operation temperature is raised, but a high operation temperature will accelerate the deactivation of the catalyst. The trade-off between operation temperature and catalyst deactivation has to be considered.

At a reformer operating temperature of 280 °C, the concentrations of hydrogen and carbon dioxide remain almost

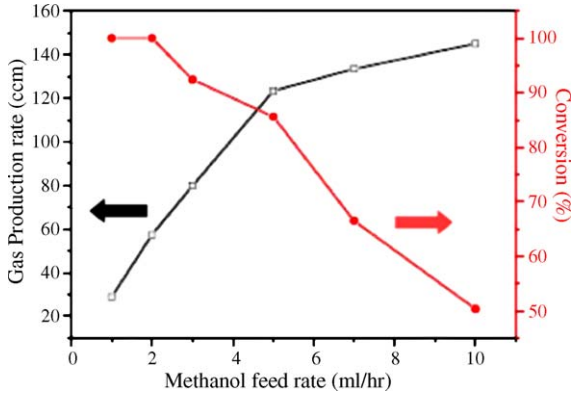

Fig. 7. Gas production rate and conversion vs. feed rate at reaction temperature of 280 °C.

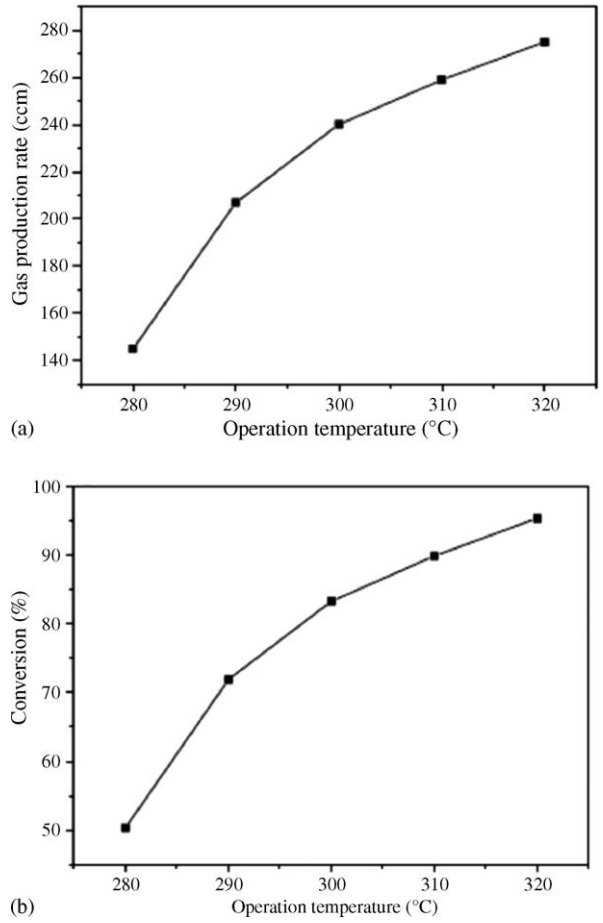

Fig. 8. Gas production rate and conversion vs. operation temperature of reformer for feed rate of 10 $cm^3\ h^{-1}$. (a) Gas production rate vs. reaction temperature at feed rate of 10 $cm^3\ h^{-1}$; (b) conversion vs. reaction temperature at the feed rate of 10 $cm^3\ h^{-1}$.

stable irrespective of the methanol feed rate, see Fig. 9. By contrast, the concentration of carbon monoxide decreases from 13,000 to 2100 ppm as the methanol feed rate increases. The reduction of carbon monoxide concentration with feed rate is closely related to the residence time. With long residence times, product gas will have an adequate time to contact the catalyst after the forward reaction, which allows the reverse reaction to occur. In this study, a long contact time

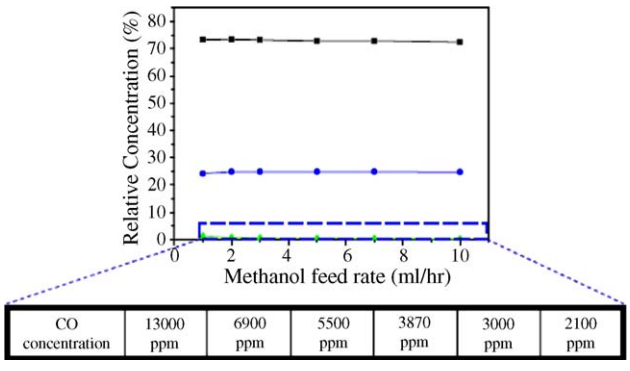

Fig. 9. Relative concentration of product gas.

of carbon dioxide results in the reverse water-gas-shift reaction, which explains the high carbon monoxide concentration at slow methanol feed rates, and the low concentration at fast methanol feed rates. The carbon monoxide concentration of 2100 ppm at a 10 $cm^3\ h^{-1}$ methanol feed rate is relatively low, but is still too high for direct application in fuel cells and has to be reduced via the preferential oxidation (PROX) reaction.

5. Conclusions

A silicon-based micro-reformer has been fabricated for portable fuel cell applications. Silicon wet etching, anodic bonding, thin-film deposition and a new catalyst loading method (fill-and-dry method) have been applied. The volume of each micro-reactor is as small as 0.55 cm^3 and the volume of the micro-reformer stack, which comprises one vaporizer and two reformers, is 15 cm^3. The gas production rate increases with the methanol feed rate and the operation temperature. The maximum hydrogen production rate is 206 cm^3 with a CO concentration of 2100 ppm. This corresponds to 20 W and the CO concentration is lower than that obtained with a conventional reformer, although it is still too high for direct application in fuel cells.

Acknowledgement

This work was supported by KOSEF through the Research Center for Energy Conversion and Storage (RCECS), Samsung SDI and the NIT Share-ISRC Program through the Inter-university Semiconductor Research Center (ISRC).

References

[1] J.P. Meyers, H.L. Maynard, J. Power Sources 109 (2002) 76–88.
[2] M. Müller, C. Müller, F. Gromball, M. Wölfle, W. Menz, Microsyst. Technol. 9 (2003) 159–162.
[3] S.C. Kelley, G.A. Deluga, W.H. Smyrl, Electrochem. Solid State Lett. 3 (2000) 407–409.
[4] J.S. Wainright, R.F. Savinell, C.C. Liu, M. Litt, Electrochem. Acta 48 (2003) 2869–2877.
[5] J. Yu, P. Cheng, Z. Ma, B. Yi, Electrochem. Acta 48 (2003) 1537–1541.
[6] J. Yu, P. Cheng, Z. Ma, B. Yi, J. Power Sources 124 (2003) 40–46.
[7] K. Shah, W.C. Shin, R.S. Besser, J. Power Sources 123 (2003) 172–181.
[8] T. Cui, J. Fang, A. Zheng, F. Jones, A. Reppnd, Sens. Actuators B Chem. 71 (2000) 228–231.
[9] S. Tanaka, K.-S. Chang, K.-B. Min, D. Satoh, K. Yoshida, M. Esashi, Chem. Eng. J. 101 (2004) 143–149.
[10] M.U. Kopp, A.J. Mello, A. Manz, Science 280 (1998) 1046–1048.
[11] J. Cheng, M.A. Shoffner, G.E. Hivichia, L.J. Kricka, P. Wilding, Nucleic Acids Res. 24 (1996) 380–385.
[12] H. Hamatsu, M. Nagase, K. Kurihara, K. Iwadate, K. Murase, Microelectron. Eng. 27 (1995) 71–74.
[13] M.A. Schmidt, Proc. IEEE 86 (1998) 1575–1585.

[14] Y. Choi, H.G. Stenger, Appl. Catal. B Environ. 38 (2002) 259–269.
[15] C.J. Jiang, D.L. Trimm, M.S. Wainwright, Appl. Catal. A Gen. 97 (1993) 145–158.
[16] F. Raimondi, K. Geissler, J. Wambach, A. Wokaun, Appl. Surf. Sci. 189 (2002) 59–71.
[17] R.S. Besser, X. Ouyang, H. Surangalikar, Chem. Eng. Sci. 58 (2003) 19–26.
[18] K. Haas-Santo, M. Fichtner, K. Schubert, Appl. Catal. A Gen. 220 (2001) 79–92.
[19] C. Agrafiotis, A. Tsetsekou, J. Eur. Ceram. Soc. 22 (2002) 423–434.
[20] B.E. Yoldas, Ceram. Bull. 54 (1974) 289.